Formation of Porous GaSb Compound Nanoparticles by Electronic-Excitation-Induced Vacancy Clustering

H. Yasuda,[1,*] A. Tanaka,[1] K. Matsumoto,[1] N. Nitta,[1] and H. Mori[2]

[1]*Department of Mechanical Engineering, Kobe University, Rokkodai, Nada, Kobe 657-8501, Japan*

[2]*Research Center for Ultra-High Voltage Electron Microscopy, Osaka University, Yamadaoka, Suita, Osaka 565-0871, Japan*

(Received 28 September 2007; published 14 March 2008)

Porous semiconductor compound nanoparticles have been prepared by a new technique utilizing electronic excitation. The porous structures are formed in GaSb particles, when vacancies are efficiently introduced by electronic excitation and the particle size is large enough to confine the vacancy clusters. The capture cross section of the surface layer in particles for the vacancies is smaller than that for the interstitials. Under the condition of supersaturation of vacancies in the particle core, porous structures are produced through the vacancy clusters to a void formation.

DOI: 10.1103/PhysRevLett.100.105506 PACS numbers: 61.80.−x, 61.46.Df, 64.70.Nd

Porous materials play an important role in the development of luminescent, catalytic, hydrogen storage materials, and so on, in which the properties can be greatly improved by a large surface-to-volume ratio [1–3]. As typical examples of the porous materials, there are zeolites [4], a porous silicon [5], sintered materials [6], foam metals [7], and so on, depending on the spatial scale of the porous structures. The nanoscale morphologies of porous structures will affect the properties in the materials. If we can prepare a porous structure not only in the bulk materials but also in the interior of individual nanoparticles, it is expected that the porous structure increases the surface area of the nanoparticles and is applicable to a capsule. Recently, methods to form a void in the interior of individual nanoparticles were found [8,9]. In these methods, the porous structures are prepared by a Kirkendall void formed during annealing of core-shell nanoparticles or oxide nanoparticles, in which the interdiffusion coefficients between two components are extremely different. The difficulties of these methods are to form core-shell nanoparticles as the starting materials, or to be limited by a combination of metallic and light elements such as oxide nanoparticles. In these methods, there is no example of a porous structure formed in III-V semiconductor compound nanoparticles. The III-V compound nanoparticles are absorbing the attention as optical or catalytic materials utilizing quantum size effects and surface effects. We consider that a preparation of porous semiconductor compound nanoparticles is particularly valuable in the enhancement of specific properties due to the large surface-to-volume ratio.

We found that phase changes take place by atom displacements when GaSb semiconductor compound nanoparticles are excited by electron beam [10–12]. Recently, it has been evident that the atom displacements and the resultant phase changes are related to the formation and migration of point defects such as vacancies and interstitials. In the present work, the formation of porous GaSb compound nanoparticles by clustering of vacancies introduced efficiently by electronic excitation and the formation mechanism has been studied by *in situ* transmission electron microscopy (TEM).

Preparation of size-controlled GaSb particles was carried out with the use of a double-source evaporator installed in the specimen chamber of an electron microscope. An amorphous carbon film was used as a supporting film and was mounted on a molybdenum grid. Using the evaporator, gallium was first evaporated from one filament to produce gallium particles on the supporting film, and then antimony was evaporated from the other filament onto the same film. The supporting film was kept at ambient temperature during the deposition. Vapor-deposited antimony atoms quickly dissolved into gallium particles to form GaSb (Ga-50 at. % Sb) compound particles [13–15]. The particles were then annealed in the microscope at 573 K for 3.6 ks and were slowly cooled to room temperature in 2.7 ks, in an attempt to homogenize the solute concentration in the particles. Electronic excitation experiments and observations were carried out using the same microscope Hitachi H-7000 TEM operating at an accelerating voltage of 25 kV. The electron flux used for excitations was 1.0×10^{20} $e\,\mathrm{m}^{-2}\,\mathrm{s}^{-1}$. The temperature of particles on the supporting films was kept at 397–430 K during the experiments. Structural changes associated with electronic excitations were observed *in situ* by bright-field images (BFIs) and selected-area electron diffraction (SAED) patterns.

An example of the structural changes in GaSb particles kept at 430 K by electronic excitation is shown in Fig. 1. Figures 1(a) and 1(a′) show a BFI of particles with the mean diameter of approximately 20 nm before excitation and the corresponding SAED, respectively. As indexed in Fig. 1(a′), the Debye-Scherrer rings can be consistently indexed as those of GaSb which has the zinc blende structure. The same area after excitation for 60 s (i.e., up to the dose of 6.0×10^{21} $e\,\mathrm{m}^{-2}$) is shown in Fig. 1(b). In the interior of the particles after the excitation, there appear voids with bright contrast. As seen from a comparison of the magnified images $\mathrm{I_a}$ and $\mathrm{II_a}$ in Fig. 1(a) with $\mathrm{I_b}$ and $\mathrm{II_b}$

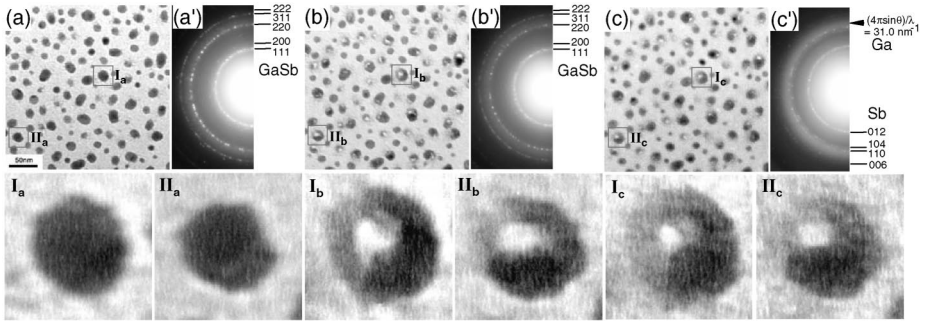

FIG. 1. An example of the structural changes in approximately 20 nm-sized GaSb particles kept at 430 K by electronic excitation. (a) A BFI and (a′) the corresponding SAED before excitation. (b) The same area after excitation for 60 s and (b′) the corresponding SAED. (c) The same area after excitation for 480 s and (c′) the corresponding SAED. The parts framed squarely are enlarged in the figures.

in Fig. 1(b), the diameter of nanoparticles after the excitation increased up to 15% compared with those before excitation. In the SAED taken after the excitation as shown in Fig. 1(b′), Debye-Scherrer rings of the zinc blende structure are recognized again. Changes in the lattice constant in GaSb particles are shown as a function of total electron dose in Fig. 2. In approximately 20-nm-sized GaSb particles kept at 430 K after excitation of the dose of 6.0×10^{21} $e\,\mathrm{m}^{-2}$, the lattice constant increased up to 1.8% compared with that before excitation. The lattice constant of GaSb particles under the same excitation condition increased up to about 2.6% with increasing dose. From the above results, it is suggested that the void swelling in the individual nanoparticles and the increase of the lattice constant of GaSb are caused by vacancies and interstitials introduced by electronic excitation, respectively.

The same area after excitation for 480 s (i.e., up to the dose of 4.8×10^{22} $e\,\mathrm{m}^{-2}$) is shown in Fig. 1(c). The voids in the individual particles change in shape and size, as seen from a comparison of the magnified images I_b and II_b in Fig. 1(b) with I_c and II_c in Fig. 1(c). In the SAED taken after the excitation as shown in Fig. 1(c′), Debye-Scherrer rings are recognized, superimposed on a weak halo ring. The Debye-Scherrer rings can be indexed consistently as those of crystalline antimony, which has the hexagonal structure. The value of the scattering vector $[K = (4\pi \sin\theta)/\lambda]$ for the halo ring is approximately 31.0 nm^{-1}, which is corresponding to the first halo of liquid gallium. This result indicates that a two-phase mixture consisting of a crystalline antimony core and a liquid gallium shell was formed in the particles. From these results, it has been evident that when GaSb particles kept at 430 K are excited by 25 keV electrons, two-phase separation takes place via void formation.

In order to see the size dependence of the porous nanoparticle formation, experiments in approximately 10-nm-sized particles kept at 397 K were carried out. An example of the behaviors of particles by the same electronic excitation condition as that in Fig. 1 is shown in Fig. 3. As seen from the comparisons of Figs. 3(a) with 3(b) and 3(a′) with 3(b′), the particle remains unchanged in both the microstructure and the SAED after excitation for 60 s. It has been noted here that such a void formation as observed after excitation in approximately 20-nm-sized particles is absent in 10-nm-sized particles. In Fig. 2, the lattice constant in 10-nm-sized particles increases with increasing dose and saturates to the value of approximately 1%. After excitation for 480 s as shown in Figs. 3(c) and 3(c′), no changes are recognized in the microstructure of the particles, but weak Debye-Scherrer rings are recognized, superimposed on a halo ring in the SAED. The most intense one of the Debye-Scherrer rings can be indexed as the 012 reflection of crystalline antimony, and the halo ring corresponds to the first halo of liquid gallium. From the result, it was evident that when 10-nm-sized GaSb particles kept at 397 K are excited by 25 keV electrons, the lattice constants of GaSb increase with increasing electron dose and two-phase separation takes place without void formation.

A candidate for a formation mechanism of the porous structures in GaSb nanoparticles predicted from the present experimental results will be discussed as follows. It is known that when the GaSb compound is excited by 25 keV electrons, many kinds of elementary excitations (i.e., inner-shell, valence, and plasmon excitations) are in-

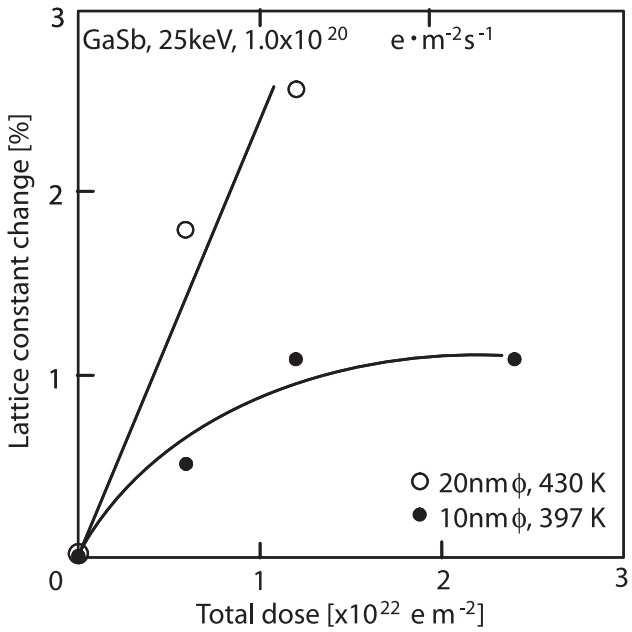

FIG. 2. Changes in lattice constants of GaSb induced by electronic excitation in nanoparticles as a function of total electron dose.

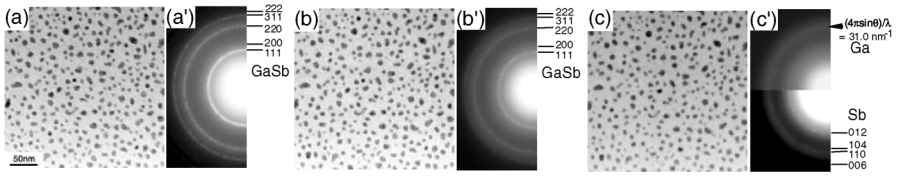

FIG. 3. An example of the structural changes in approximately 10-nm-sized GaSb particles kept at 397 K by electronic excitation. (a) A BFI and (a′) the corresponding SAED before excitation. (b) The same area after excitation for 60 s and (b′) the corresponding SAED. (c) The same area after excitation for 480 s and (c′) the corresponding SAED.

duced. The primary excitation energy of the incident electrons ranges roughly double the energy of gallium K shell 10.4 keV, but deviates from the energy of antimony K shell 30.5 keV [16]. On the other hand, the excitation probability of L shells of gallium and antimony is relatively low, since the energy of the incident electrons is approximately 1 order of magnitude higher than the L shell energies ranging from 1.1 to 4.7 keV [16]. In the present case, the probability of the gallium K shell excitation which satisfies the resonance excitation condition is largest in all the elementary excitations. Nearly half of the competitive relaxation processes (i.e., Auger emission and x-ray fluorescence) to the primary gallium K shell excitation is the Auger transition in which the transition probability is 0.47 [17]. Consequently, the final two-hole states in the valence band are formed by the predominant primary K shell or low-efficient primary L shell Auger transitions. The two-hole states will play an important role in the atom displacements. An atom which has a minimum energy in the electronic ground state is excited to a high energy state due to the increase of the adiabatic interatomic potential under the presence of the two-hole states [18–21]. The excited atom displaces from the equilibrium site to relax the energy of the system and to deexcite to the ground state for a short lifetime. In this stage, the bond breaking takes place, and the excess energy accumulated by the relaxation converts directly into the atomic kinetic energy. When the sum of the kinetic energy and thermal energy is larger than the energy barrier to move from the atomic site immediately after the deexcitation, the displaced atom can form a point defect in the crystal. High density of point defects is introduced under the presence of high density of electronic-excitation-induced atom displacements and enhances the formation of defect clusters and atomic diffusion.

In nanoparticles, such an electronic excitation effect becomes remarkably efficient. The final two-hole states which have short lifetimes of 10^{-15} to 10^{-12} s decay by the scattering with electrons in the solid [22]. The lifetimes of the excited states near the valence band maximum or the Fermi level become long by decreasing the densities of states. In nanoparticles, a lot of surface and defect states are formed due to the high surface-to-volume ratio, and high vibrational states are induced by the lattice softening [23–25]. The energy levels are broadened by fluctuations of such defective bonds. Additionally, the penetrations of the energy levels from the valence band maximum into the forbidden gap take place due to the electron-phonon scattering enhanced by the lattice softening [26]. Consequently, the densities of states in nanoparticles which have the defective bonds and softened lattices will become lower than those in the perfect crystalline bulk solids. The low electron densities make the lifetimes of the excited states formed in nanoparticles longer in comparison with those in the bulk solids. The long lifetimes of the excited states, that is, pinning of the excited states, increase the energy gain by the relaxation, and the resultant atom displacements are enhanced. On the other hand, the shallow interatomic potentials due to the lattice softening in nanoparticles reduce the activation energy for the atomic diffusion [27,28]. The increase of the energy gain by the long excitation lifetime and the low activation energy for the diffusion will make it easy to displace the excited atoms in nanoparticles.

Through the present experiments, it has become evident that vacancies and interstitials introduced efficiently by electronic excitation in nanoparticles act as a trigger for the void formation and phase separation. It was confirmed from previous experiments that optical excitation of the clean GaAs and GaP surfaces can lead to emission of neutral gallium atoms, since in the presence of electron-hole excitations the adiabatic potential energy surface for the gallium atoms becomes antibonding which causes their desorption [29–33]. On the other hand, it is possible to conclude that the radiation induced defects which are stable at room temperature in GaAs are most likely simple native defects such as vacancies, interstitials, or antisite defects [34]. It is speculated from these previous results that gallium atoms on the lattice points are displaced by excitation to form gallium interstitials in the crystal.

When vacancies and gallium interstitials become mobile and apart from annihilation by recombination, they contribute to the growth of defect clusters. The interstitials and their clusters (i.e., interstitial dislocation loops at the early stage) have a strong compressive strain field and the compressive strain field interacts more strongly with a tensile strain field of the surface layer of the particle than with strain fields of an individual defects or their clusters. The surface layer of the particle will act as a preferential sink for interstitials and their clusters over the whole particles. The result of this greater capture cross section of the surface layer for interstitials and their clusters is to create a situation where the vacancies are the dominant species in

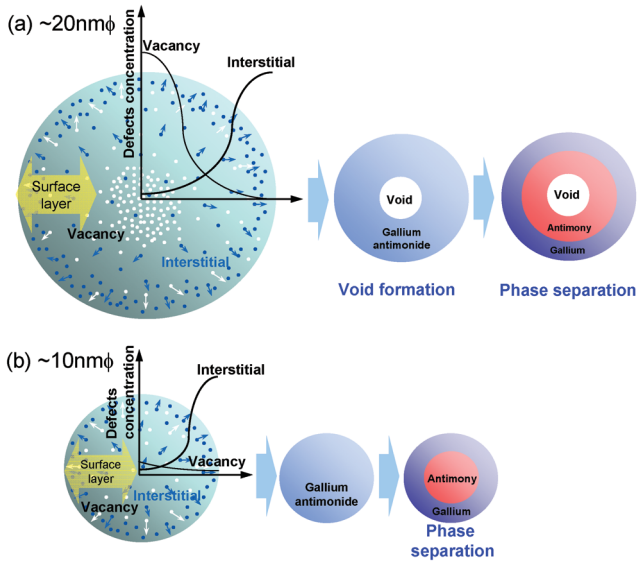

FIG. 4 (color). Schematic illustrations of defect migrations and defect concentrations as a function of distance from the center of a nanoparticle and the behaviors of the structural changes. The particle sizes are approximately 20 nm and 10 nm in (a) and (b), respectively.

the particle. On the other hand, the capture cross section of the surface layer for vacancies and their clusters is smaller than that for interstitials and their clusters. The vacancies and their clusters interact weakly with that of the surface layer. In nanoparticles, only the vacancies in the surface layer which is finite in thickness can disappear toward the top of the surface.

Figure 4 shows schematic illustrations of defect migrations and defect concentrations as a function of distance from the center of a nanoparticle and the structural changes. As shown in Fig. 4(a), in approximately 20-nm-sized particles, the vacancy concentration in the particle core is higher than that in the surface layer, but interstitial concentration increases toward the surface. Consequently, under the condition of vacancy supersaturation in the particle core the vacancy clusters will grow to form a void, and the subsequent surface segregation of interstitial clusters will bring about the separation to the two-phase structure.

This mechanism also gives an explanation for size dependence of electronic-excitation-induced porous structure formation. In approximately 20-nm-sized particles, vacancies and their clusters near the surface layer annihilate, but vacancy supersaturation in the particle core brings about the void formation. On the other hand, in approximately 10-nm-sized particles, vacancy concentration is low over the whole particle which corresponds to the surface layer, and no void formation takes place as illustrated in Fig. 4(b). In either case, the surface segregation of interstitials will cause the phase separation in nanoparticles.

In conclusion, we have prepared a porous structure in semiconductor compound nanoparticles by a new technique utilizing electronic excitation. When clustering of vacancies introduced by electronic excitation is controlled efficiently and the particle size is large enough to confine the vacancy clusters, the porous structures are formed in nanoparticles.

*Corresponding author.
yasuda@mech.kobe-u.ac.jp

[1] N. Herron *et al.*, J. Am. Chem. Soc. **111**, 530 (1989).
[2] G. D. Stucky and J. M. Dougall, Science **247**, 669 (1990).
[3] T. Inui, S. Phatanasri, and H. Matsuda, J. Chem. Soc. Chem. Commun. 205 (1990).
[4] W. M. Meier and D. H. Olson, *Atlas of Zeolite Structure Types* (Butterworth-Heine-mann, London, 1992), p. 12.
[5] L. T. Canham, Appl. Phys. Lett. **57**, 1046 (1990).
[6] V. T. Morgan, Powder Metall. **12**, 426 (1969).
[7] H. Nakajima, T. Ikeda, and S. K. Hyun, Adv. Eng. Mater. **6**, 377 (2004).
[8] Y. Yin *et al.*, Science **304**, 711 (2004).
[9] R. Nakamura, J.-G. Lee, D. Tokozakura, H. Mori, and H. Nakajima, J. Appl. Phys. **101**, 074303 (2007).
[10] H. Yasuda, H. Mori, and J. G. Lee, Phys. Rev. Lett. **92**, 135501 (2004).
[11] H. Yasuda, H. Mori, and J. G. Lee, Phys. Rev. B **70**, 214105 (2004).
[12] H. Yasuda *et al.*, Eur. Phys. J. D **37**, 231 (2006).
[13] H. Yasuda and H. Mori, Phys. Rev. Lett. **69**, 3747 (1992).
[14] H. Yasuda and H. Mori, Z. Phys. D **31**, 131 (1994).
[15] H. Yasuda and K. Furuya, Eur. Phys. J. D **10**, 279 (2000).
[16] K. Way *et al.*, At. Data Nucl. Data Tables **20**, 311 (1977).
[17] W. Bambynek *et al.*, Rev. Mod. Phys. **44**, 716 (1972).
[18] H. Sumi, Surf. Sci. **248**, 382 (1991).
[19] D. E. Ramaker, C. T. White, and J. S. Murday, Phys. Lett. **89A**, 211 (1982).
[20] A. Yasui, T. Uozumi, and Y. Kayanuma, Phys. Rev. B **72**, 205335 (2005).
[21] N. Itoh and T. Nakayama, Phys. Lett. **34**, 953 (1975).
[22] R. Weissmann and K. Muller, Surf. Sci. Rep. **1**, 251 (1981).
[23] J. Harada and K. Ohshima, Surf. Sci. **106**, 51 (1981).
[24] K. Ohshima, T. Yoshiyama, and J. Harada, J. Phys. C **18**, 3073 (1985).
[25] U. Buck and R. Krohne, Phys. Rev. Lett. **73**, 947 (1994).
[26] J. P. Walter *et al.*, Phys. Rev. Lett. **24**, 102 (1970).
[27] L. D. Marks and P. M. Ajayan, Ultramicroscopy **20**, 77 (1986).
[28] P. M. Ajayan and L. D. Marks, Phys. Rev. Lett. **60**, 585 (1988).
[29] K. Hattori *et al.*, Phys. Rev. B **45**, 8424 (1992).
[30] J. Kanasaki *et al.*, Phys. Rev. Lett. **70**, 2495 (1993).
[31] J. Singh, N. Itoh, Y. Nakai, J. Kanasaki, and A. Okano, Phys. Rev. B **50**, 11 730 (1994).
[32] O. Pankratov and M. Scheffler, Phys. Rev. Lett. **75**, 701 (1995).
[33] G. A. Samara, D. W. Vook, and J. F. Gibbons, Phys. Rev. Lett. **68**, 1582 (1992).
[34] H. C. Snyman and J. H. Neethling, Radiat. Eff. **69**, 199 (1983).